

Effect of Cu(II) ligands on electroless copper deposition rate in formaldehyde solutions: An EQCM study

R. PAULIUKAITĖ¹, G. STALNIONIS¹, Z. JUSYS² and A. VAŠKELIS^{1,*}

¹Department of Catalysis, Institute of Chemistry, Goštauto 9, LT-01108, Vilnius, Lithuania

²Department of Surface Chemistry and Catalysis, University of Ulm, 89069, Ulm, Germany

(*author for correspondence e-mail: vaskelis@ktl.mii.lt)

Received 30 August 2005; accepted in revised form 5 May 2006

Key words: copper, copper(II) complexes, electroless deposition, EQCM, formaldehyde

Abstract

The electroless copper deposition rate for 6 Cu^{II} complexes decreases in the ligand sequence: nitrilotriacetic acid (NTA) > *N,N,N',N'*-tetrakis-(2-hydroxypropyl)-ethylenediamine (Quadrol) > glycerol > L(+)-tartrate ~ sucrose > DL(±)-tartrate. Both Cu^{II} complex stability and specific ligand effects were found to influence the Cu deposition process. The specific ligand effects are most obvious in the case of Quadrol (high kinetic activity at a high Cu^{II} complex stability), glycerol and sucrose (additional reaction of Cu₂O formation by interaction of Cu^{II} with ligand). According to the EQCM data for 11 Cu^{II} complexes (including data from the former study) the higher kinetic activity is demonstrated by complexes with ligands containing amino groups; this factor is more important for Cu deposition rate than copper complex stability. A potential dependence of the Cu reduction partial current on the electrode potential has been extracted from the EQCM data in the complete electroless plating bath. An increase in Cu^{II} reduction rate was found to occur in electroless plating solution for Cu^{II} complexes with NTA and Quadrol compared with that in formaldehyde-free solutions. Possible reasons for the acceleration of the partial Cu^{II} reduction reaction and the overall process kinetics are discussed using a hypothetical reaction sequence involving intermediate copper oxy-species and active Cu* formation as well as development of the preferred Cu surface structure.

1. Introduction

Electroless copper deposition is widely used for the formation of metallic copper layers on plastics and other dielectrics, semiconductors and other materials for the production of printed and integrated circuits, etc. [1–3]. Autocatalytic reduction of Cu^{II} by formaldehyde, which is usually used for electroless copper deposition, can be generally expressed as the coupling of two partial electrochemical reactions: anodic formaldehyde (methyleneglycol anion) oxidation and cathodic Cu^{II} (chelated by ligands) reduction. This view, proposed almost four decades ago [4–6], is well supported by experimental evidence [1–3, 7, 8]. The mixed potential (E_m) is attained at equal rates (currents) of both partial reactions under open-circuit conditions. Either a negative or a positive shift of the electrode potential results in the net current, which is equal to the algebraic sum of the partial currents.

Therefore, additional non-electrochemical techniques are required to study the potential dependences of individual reactions in a complete electroless deposition bath. A combination of on-line mass spectrometry (MS) with cyclic voltammetry (CV) or other potential programs called differential electrochemical mass

spectrometry (DEMS) [9] was used to monitor the formaldehyde oxidation (hydrogen evolution) rate in electroless copper plating solution [10–12].

Figure 1(a) shows an example of partial current extraction during electroless copper plating as a function of electrode potential using a thin-layer DEMS flow-cell [12]: hydrogen evolution during formaldehyde oxidation on Cu electrode was measured on-line by MS and was converted into the partial formaldehyde oxidation current (circles) using a calibration constant for cathodic hydrogen evolution on the same electrode. As a result, the partial current for Cu^{II} reduction to copper metal (dotted line) can be easily calculated as the difference between the net current (solid line) and measured formaldehyde oxidation partial current (circles).

Similarly, partial reaction currents in electroless copper plating solution can be extracted using electrochemical quartz crystal microgravimetry (EQCM) to *in situ* monitor the rate of copper deposition under open-circuit conditions and as a function of the electrode potential [13–19]. Figure 1b shows the measured copper deposition rate converted to the partial Cu^{II} reduction current (dotted line) using the EQCM calibration constant for cathodic Cu deposition, and the

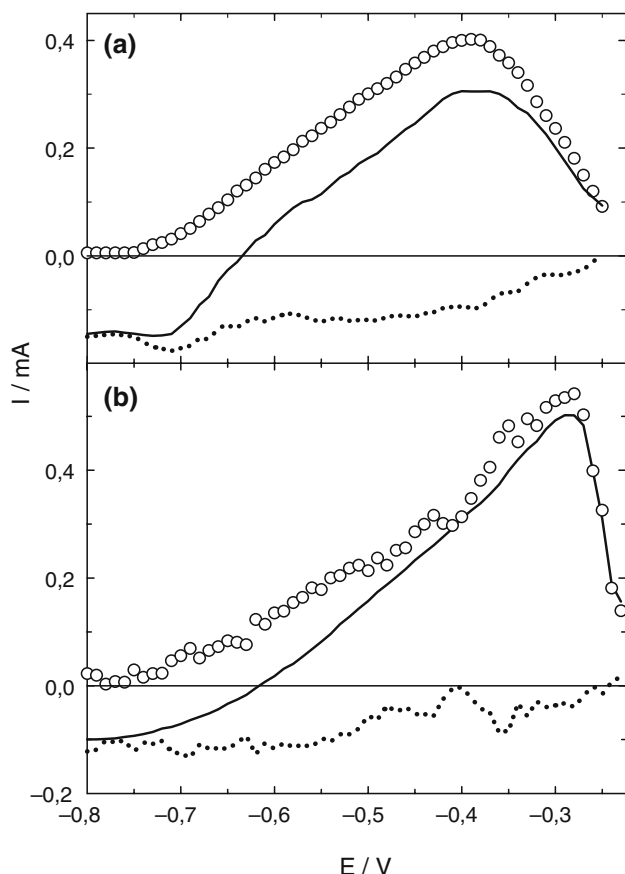


Fig. 1. Dependence of faradaic current (—), and partial currents for formaldehyde oxidation (ooo) and Cu^{II} reduction (...) found from DEMS flow-cell (a) and EQCM (b) measurements. Solution contained (mol l^{-1}): CuSO_4 – 0.008; EDTA- 0.04; CH_2O – 0.02; pH 13; $t^\circ = 20 \pm 1^\circ\text{C}$.

partial formaldehyde oxidation current (circles), calculated as the difference between the net current (solid line) and partial Cu^{II} reduction current (dotted line) according to results presented in [13]. Clearly, despite differences in the DEMS and EQCM cell designs, working electrodes and forced electrolyte convection (used in DEMS measurements), the partial anodic and cathodic currents for electroless copper deposition found using these two techniques are fully complementary and are in good qualitative and quantitative agreement. A combined DEMS/EQCM approach was introduced recently [20], allowing simultaneous detection of both gaseous and solid phases at electroless metal deposition.

Acceleration of the cathodic half-reaction [7] or of both partial reactions [16] during electroless copper deposition was found. This cannot be explained in terms of the coupling of independent electrochemical reactions according to mixed potential theory. EQCM was employed in our previous work [14] for a comparative study of the Cu^{II} reduction rate in both formaldehyde-free and complete electroless copper plating solutions containing various EDTA-type compounds as chelating agents for Cu^{II} . The data obtained supported mechanistic considerations explaining both partial reaction interaction and copper complex composition/structure effects.

Complexing of Cu^{II} by suitable ligand is important in traditional formaldehyde-containing alkaline electroless copper plating baths. The compounds used as ligands should form Cu^{II} complexes stable enough to prevent $\text{Cu}(\text{OH})_2$ formation and precipitation – the concentration of “free” (uncomplexed) Cu^{II} ions in the pH range 11–14 should not exceed 10^{-12} – 10^{-18} M, respectively.

EDTA (ethylenediaminetetraacetic acid) is currently the most widely used ligand in systems for electroless copper plating [1–3]. In practical applications Quadrol (*N,N,N',N'*-terakis-(2-hydroxypropyl)-ethylenediamine) and tartrates, both natural L(+)-tartrate (Rochelle salt) and synthetic DL(–)-tartrate, also are frequently used. For some time glycerol was widely employed as Cu^{II} ligand in electroless copper plating solutions [21–23].

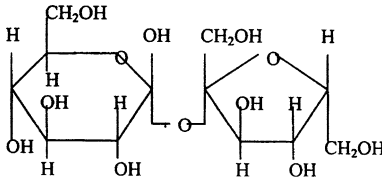
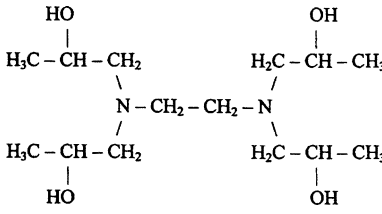
In this work the EQCM investigations of autocatalytic Cu^{II} reduction by formaldehyde were continued following the approach used previously [14]. The copper complexes studied in this work contained ligands of different structure, including EDTA-type aminopolycarboxylate-nitrilotriacetate (NTA), hydroxypolyamine-Quadrol, hydroxycarboxylates-tartrates, polyhydroxylic compounds – glycerol and sucrose. The structure of the ligands employed in this study, the corresponding Cu^{II} complexes, their stability constants, complex distribution and calculated reversible potential of Cu – Cu^{II} couple are listed in Table 1. The equilibrium potential of copper in the solutions studied shifts to more negative values by 0.11 V going from NTA and sucrose to Quadrol, the free copper ion concentration decreasing by almost 4 orders. The complexation level of Cu^{II} in this solution group is lower compared to that studied earlier [14], where E_c values were in the range from –0.27 to –0.36 V. The entire group of 11 Cu^{II} complexes studied presents a sequence of solutions where Cu^{II} complexation (free Cu^{II} ion concentration) changes by more than 7 orders (E_c shifts by 0.22 V).

2. Experimental

EQCM experiments were performed in a way similar to that described earlier [14, 29]. AT-cut quartz crystals of 6 MHz fundamental frequency (from Intelemetrics Ltd., UK) sputtered by gold from both sides were used. They were connected to a home-built oscillator. Their electrochemically and piezoelectrically active geometric areas were 0.636 and 0.283 cm^2 , respectively. Quartz crystals were installed at the bottom of the cell of working volume ca. 2 ml. The upper part of the cell contained the Pt-wire counter electrode, joints for the electrolyte inlet and the Luggin capillaries, and the electrolyte outlet tube. The construction of the cell allowed exchange of the solution under controlled electrode potential [30]. The electrolytes in the supply bottles were constantly purged with Ar.

Prior to the experiments a copper layer was electro-deposited onto a gold sublayer on quartz crystal

Table 1. Complexing agents, corresponding Cu^{II} complexes, their stability constants [24–28], complex distribution and equilibrium potential of Cu–Cu^{II} couple

Structure of complexing agent	Complexing agent	Complexes	log β	E _c /V
$\begin{array}{c} \text{CH}_2 - \text{COOH} \\ \\ \text{N} - \text{CH}_2 - \text{COOH} \\ \\ \text{CH}_2 - \text{COOH} \end{array}$	NTA – nitrilotriacetic acid	– CuX(OH) ²⁻ 100 % (X ³⁻ – NTA anion)	– 16.3	–0.14
	Succhrose	CuSa(OH) ₂ ⁻ 10% CuSa(OH) ₃ ²⁻ 50% CuSa ₂ (OH) ₂ ²⁻ 40% (Sa ⁻ – succhrose anion)	17.6 19.4 19.6	–0.14
$\begin{array}{c} \text{CH}_2 - \text{OH} \\ \\ \text{CH} - \text{OH} \\ \\ \text{CH}_2 - \text{OH} \end{array}$	Glycerol	CuGl(OH) ₃ ²⁻ 20% CuGl(OH) ₂ ²⁻ 80% (Gl ⁻) – glycerol anion	20.2 21.1	–0.17
$\begin{array}{c} \text{HOOC} \quad \text{COOH} \\ \diagdown \quad / \\ \text{H} - \text{C} - \text{C} - \text{OH} \\ / \quad \diagdown \\ \text{HO} \quad \text{H} \end{array}$	L(+)-tartaric acid DL(±)-tartaric acid	CuT(OH) ₂ ³⁻ 5% CuT ₂ ⁴⁻ 80% CuT ₂ (OH) ₂ ⁶⁻ 15% (T ³⁻ (±) – tartrate anion)	18.2 20.8 21.8	–0.18
	N,N,N',N'-tetrakis- (hydroxypropyl)- ethylenediamine or quadrol	CuQ(OH) ₂ 80% CuQ ₂ (OH) ₂ 20% (Q – quadrol)	26.9 29.1	–0.25

mounted in the cell from a solution containing 1.0 mol l⁻¹ CuSO₄ and 0.5 mol l⁻¹ H₂SO₄ at a current density of 10 mA cm⁻² for 15–20 s.

EQCM measurements were carried out using a precision frequency counter Ch3-64 and two digital voltmeters B7-46 connected to a PC trough an IEEE 488 interface (all the equipment was made in Russia). A programming potentiostat PI-50-1 and a sweep generator PR-8 (Russia) were used to control the electrode potential. The potential was measured with respect to an Ag/AgCl/KCl_{sat} reference electrode and is given below vs. a standard hydrogen electrode (SHE). The electrode potential, the faradaic current and the frequency measured (counted with an accuracy of 0.01 Hz) were transferred to the PC every 1.3 s. Differential EQCM data (the frequency change rate df/dt) were found as the difference between two frequency measurements per 1 s. A calibration constant 33.5 Hz s⁻¹ per 1 mA was found in EQCM measurements of copper deposition from alkaline Cu(II) solutions containing various ligands in most cases (except some higher values for glycerol and sucrose) and was used to convert the counted frequency to current units in the complete electroless copper

plating solution. A partial current of formaldehyde oxidation in electroless plating solutions was found as the difference between the net current and that detected from EQCM data (see Figure 1(b)).

The solution contained (mol l⁻¹): CuSO₄, 0.008 or 0.0; ligand: NTA, sucrose, glycerol, L(+)-tartrate and DL(±)-tartrate, 0.04 or 0.032; Quadrol 0.02 or 0.012; CH₂O, 0.02 or 0.0; pH 13.0; $t^{\circ} = 20 \pm 1^{\circ}\text{C}$. Analytical grade chemicals and triply distilled water were used to prepare the solutions.

3. Results and discussion

3.1. The EQCM study of electroless copper deposition rate under open-circuit conditions

The kinetics of electroless copper deposition under open-circuit conditions and the corresponding values of the mixed potential for the initial period of the process (5 min) are given in Figure 2(a, b). The highest rate of electroless copper deposition is obtained in NTA solutions at the most positive E_m values, while it is the lowest

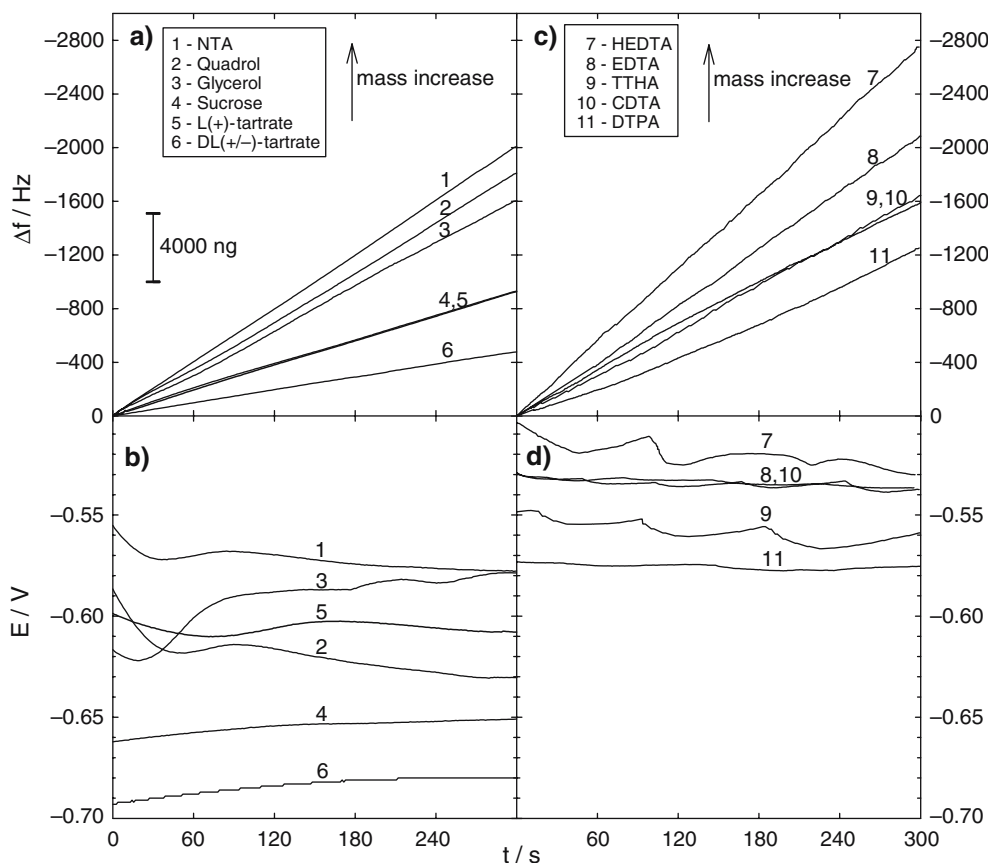


Fig. 2. Kinetics of electroless copper plating – (a) and (c), open-circuit potential – (b) and (d), measured by EQCM. Solution contained (mol l^{-1}): $\text{CuSO}_4 - 0.008$; complexing agent – 0.04 except Quadrol – 0.02; $\text{CH}_2\text{O} - 0.02$; pH 13; $t^\circ = 20 \pm 1^\circ \text{C}$. The data of (c) and (d) from [14].

in DL(–)-tartrate solutions at the most negative E_m . The copper deposition rate decreases in the ligand sequence: NTA > Quadrol > glycerol > L(+)-tartrate \sim sucrose > DL(–)-tartrate, the difference between the first 3 ligands being not so large. Though the highest copper deposition rate is found in the solution of a rather low Cu^{II} complexation (Cu–NTA complex) the close rate value is obtained in the solution of the highest complexation (Cu–Quadrol complex), consequently, the Cu^{II} complexation is not the main factor determining the electroless copper deposition process rate.

Combining data of the present study with those of [14] (Figure 2c, d) we obtain the following sequence of ligands according to autocatalytic reduction rate decrease for corresponding Cu^{II} complexes: HEDTA (hydroxyethylenediamine triacetic acid) > EDTA \sim NTA > Quadrol > glycerol > CDTA (trans-cyclohexane-1,2-diamine tetraacetic acid) \sim TTHA (triethylenetetraamine hexaacetic acid) > DTPA (diethylenetriamine pentaacetic acid) > L(+)-tartrate \sim sucrose > DL(–)-tartrate, the overall rate change being approx. 7-fold. It is necessary to note that the ligand sequence may depend on solution pH due to different rate dependence on pH for various complexes; e.g. at lower solution alkalinity the copper deposition rate from DL(–)-tartrate solutions exceeds that from L(+)-tartrate ones [31].

The more positive E_m values correspond, as a rule, to the higher plating rates; the relationship has been found in [14] also (Figure 2). Both E_m and process rate values are determined by the electrochemical characteristics of coupled partial reactions. As is evident from the electrochemical data presented below, the result of the partial reactions coupling depends mostly on the characteristics of cathodic copper deposition process which is more sensitive to the nature of the ligand than anodic formaldehyde oxidation. The decrease in the rate of electroless copper deposition in solutions with E_m value becoming more negative corresponds to a negative shift of the $\text{Cu}^{\text{II}}/\text{Cu}$ potential due to the increase in the pK value of the Cu^{II} complexes as well as due to kinetic factors. On the other hand, in Quadrol solutions E_m is more positive and the copper plating rate is higher compared to those of less stable tartrate complexes (Table 1, Figure 2).

The variations in electroless deposition rate in some cases can be explained by changes in the surface morphology, e.g. the roughness factor, in the course of electroless plating. The latter was found to depend on the Cu^{II} ligand in earlier studies of EDTA, Quadrol and tartrate solutions of electroless copper plating [31, 32].

The origin of electrode mass change in glycerol and sucrose-containing electroless plating solutions differs from that in other solutions. As mentioned in the

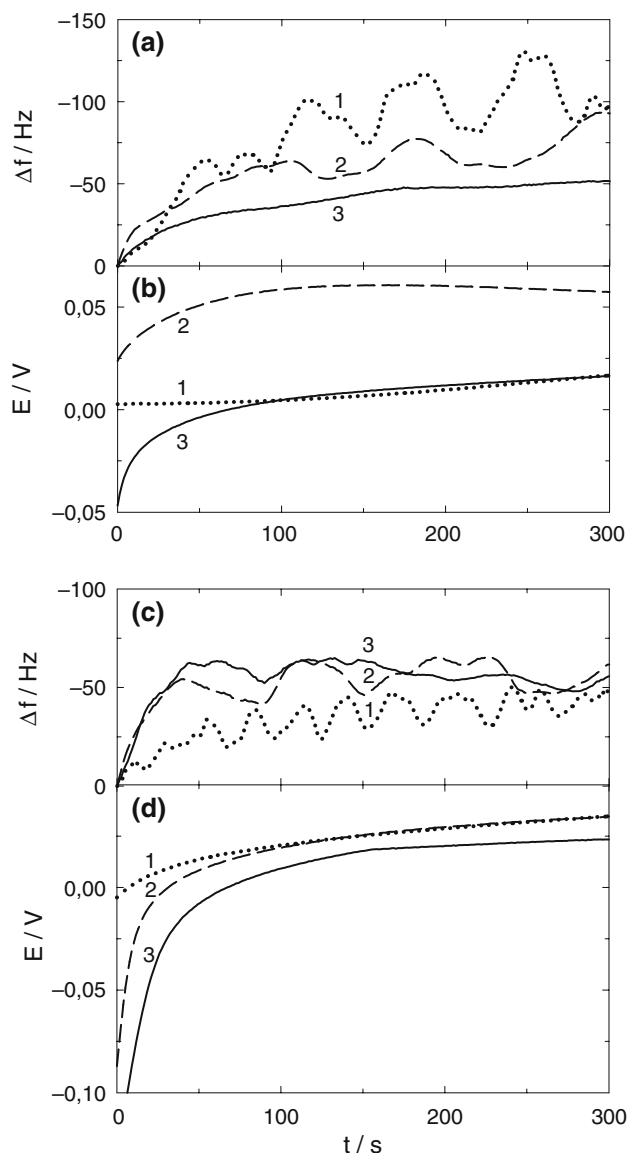


Fig. 3. Kinetics of copper electrode mass change [(a) and (c)] and corresponding open-circuit potential [(b) and (d)] in Cu^{II} -glycerol [(a) and (b)] and Cu^{II} -sucrose [(c) and (d)] formaldehyde-free solutions measured by EQCM. Solution contained (mol l^{-1}): $\text{CuSO}_4 = 0.008$; complexing agent: 0.005 (1); 0.01 (2), 0.02 (3); pH 12.5; $t^\circ = 20 \pm 1^\circ \text{C}$.

experimental section, the higher EQCM calibration constant values indicate additional reactions (possibly, deposition of mixed Cu and Cu_2O layer) occurring during electrochemical and electroless copper deposition. This was confirmed by a mass gain found at equilibrium potential of the $\text{Cu}^{\text{II}}/\text{Cu}$ couple.

The EQCM measurements showed copper electrode mass build-up in alkaline Cu^{II} -glycerol and Cu^{II} -sucrose formaldehyde-free solutions under open-circuit conditions, suggesting reduction of Cu^{II} ions by glycerol and sucrose (Figure 3). The electrode mass increased quickly in the first 10 s. Later the mass gain was slower or stopped. In several cases the electrode mass changed periodically – increasing and decreasing with time. The most distinct electrode mass oscillations were observed

at lower ligand concentration (0.005 M), their period being 10–50 s. The open-circuit potential shifted to more positive values in the initial period, and attained a steady value in the range 0.0–0.05 V. Self-oscillating Cu^{II} -lactate and Cu^{II} -tartrate systems, resulting in layered copper/cuprous oxide composites, were studied by confocal Raman spectroscopy at lower pH values (10.5) [33].

The electrode mixed potential values in these solutions (Figure 3b, d) are located in the Cu_2O stability area and suggest an explanation of the process observed as an interaction of the ligand and Cu^{II} with formation of Cu_2O (note some higher calibration constant values for Cu electrodeposition from glycerol and sucrose solutions). The easy spontaneous formation of Cu_2O in glycerol-containing electroless copper plating solutions is well known [34]. The periodic phenomena related to Cu_2O formation (Cu surface passivation) were also observed in electroless copper plating solutions containing Cu^{II} -glycerol complex [35].

3.2. Partial copper deposition reaction in formaldehyde-free and electroless copper plating solutions

EQCM data for alkaline Cu^{II} and electroless copper plating solutions containing different complexing agents are shown in Figures 4–8. A partial current of copper deposition and dissolution was found by converting the frequency change rate of the quartz crystal to current units using the calibration constant $33.5 \text{ Hz s}^{-1} \text{ mA}^{-1}$ found from the frequency and current data of copper deposition and dissolution in the absence of formaldehyde. Such a conversion was not done for the glycerol and sucrose solutions: the calibration constant showed considerable deviations from the theoretically expected value and depended on potential, indicating that the copper deposition process in these solutions is complicated by additional reactions, *e.g.* Cu_2O formation (see below). A higher noise in the EQCM data in electroless plating solution compared with formaldehyde-free solutions is due to the formation of gas (hydrogen) bubbles in the course of electroless plating [13, 14].

EQCM curves obtained in solutions containing Cu^{II} complexes under study are similar to those obtained in the earlier work [14] except for two ligands, glycerol and sucrose. In their solutions the mass build-up is observed even at the reversible $\text{Cu}/\text{Cu}^{\text{II}}$ potential (Figure 4).

For the other 4 ligands formation of Cu_2O occurs at ca. -0.2 V in the positive-going scan and reduction of the Cu_2O formed is achieved at ca. -0.4 V in the negative-going scan. The df/dt response for Cu_2O formation and reduction is small, compared to the current, due to a rather small mass change in the $\text{Cu}-\text{Cu}_2\text{O}$ transition.

The irreversibility of the $\text{Cu}^{\text{II}}/\text{Cu}$ couple in the solutions under study should be noted: the difference between the potential of Cu^{II} reduction and that of Cu anodic dissolution is in the range 0.15–0.4 V (Table 2) and is lower compared to the EDTA-type ligands [14].

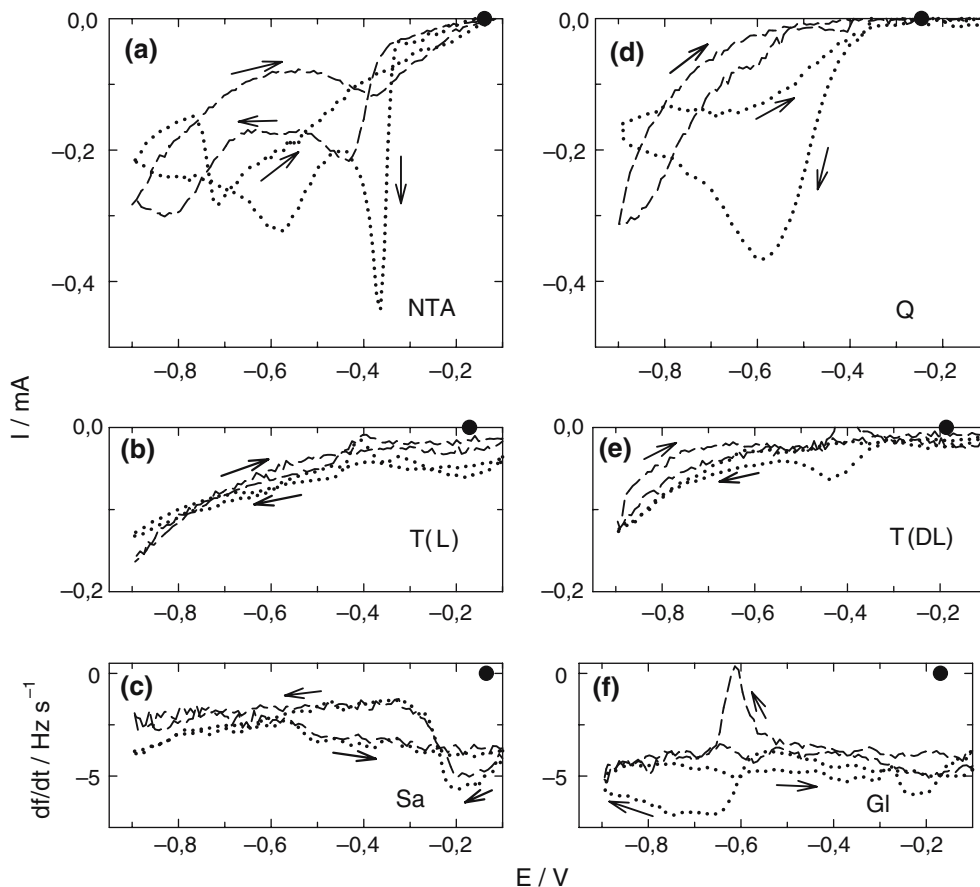
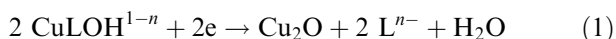


Fig. 4 Dependence of copper deposition rate on potential. [(a)-(d)] – faradaic current calculated from EQCM data, (e) and (f) – frequency change rate in formaldehyde-free Cu^{II} (---) and electroless copper plating (...) solutions. Complexing agent: (a) NTA, (b) Quadrol, (c) L(+)-tartrate, (d) DL(±)-tartrate, (e) sucrose, (f) glycerol. (*) – calculated equilibrium $\text{Cu}^{\text{II}}/\text{Cu}$ potential.

The rate of cathodic copper deposition and anodic dissolution depends on the nature of the ligands used.

A comparison of the electrochemical behaviour of Cu^{II} complexes was carried out taking into account their E_c (Table 1) and overvoltage values. Cathodic copper deposition begins most easily in NTA solutions. The overvoltage for obtaining a Cu deposition rate equivalent to -0.5 Hz s^{-1} frequency change rate is the lowest, the overvoltage for tartrates and Quadrol being considerably higher. The overvoltage has a tendency to increase with increasing Cu^{II} complexation: the data for NTA and Quadrol illustrate this well (Table 2).

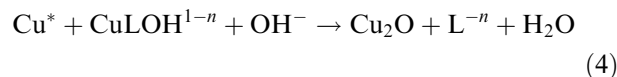
The hypothetical mechanism of cathodic copper deposition with formation of inter-mediate Cu^{I} oxy-species (Cu_2O), in the course of the reduction of a $\text{Cu}^{\text{II}}\text{-L-OH}$ complex [14] also seems to be appropriate in this work. Thus, reduction of Cu^{II} monohydroxy complexes Cu-LOH^{1-n} (where L^{n-} is the ligand anion) to copper metal via intermediate Cu_2O is assumed as the main Cu deposition route in the potential region -0.5 to -0.8 V :



Freshly deposited copper atoms either incorporate into the crystalline lattice



or react with CuLOH^{1-n} , due to their high reactivity, leading to formation of intermediate Cu_2O as an alternative route to the slow reaction (1)



Such a hypothetical reaction sequence was deduced from EQCM studies of the kinetic H/D isotope effect during $\text{Cu}^{\text{II}}\text{-EDTA}$ complex reduction to copper metal [13].

Cu^{II} in NTA solution exists entirely in the form of the hydroxy complex at pH 13 (Table 1) and cathodic copper deposition from this solution is the most easy in the group of complexes studied: the overvoltage is the lowest and comparatively high current is obtained in the potential range -0.5 to -0.6 V (Figure 2). On the other hand, no increase in copper deposition rate occurs in this potential region in other Cu^{II} solutions containing no monohydroxy complexes.

Cu^{II} reduction to copper metal in electroless copper plating solution in the negative-going potential scan

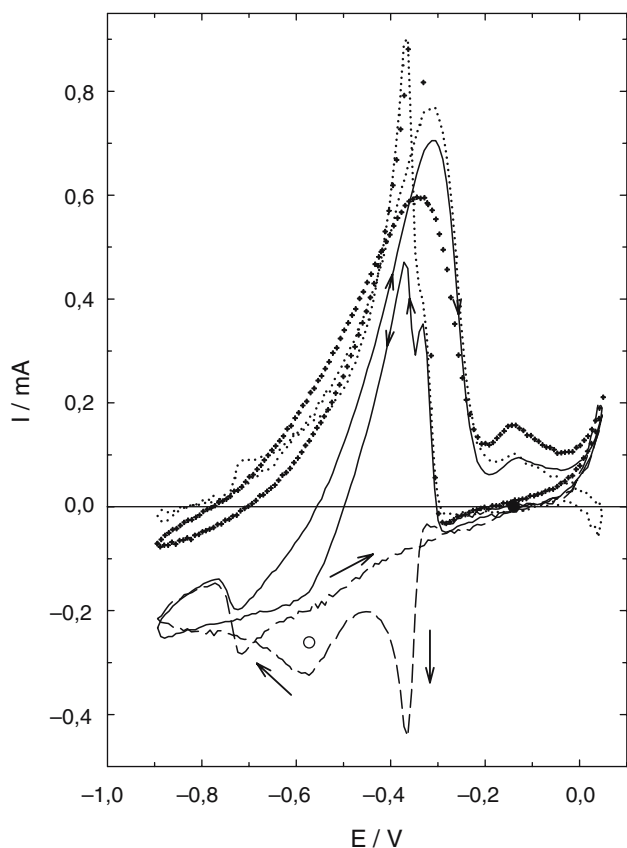


Fig. 5. Dependence of faradaic current [measured directly (—), calculated from EQCM data (- - -), and found from their difference (...)] on copper electrode potential. Solution contained (mol l^{-1}): $\text{CuSO}_4 - 0.008$; $\text{NTA} - 0.04$; $\text{CH}_2\text{O} - 0.02$; $\text{pH } 13$; $t^\circ = 20 \pm 1^\circ\text{C}$. (o) – fradaic current measured directly in Cu^{II} -free 0.02 mol l^{-1} formaldehyde solution containing 0.032 mol l^{-1} of NTA; (O) – instantaneous copper deposition rate measured by EQCM under open-circuit conditions.

begins at potentials close to the equilibrium value for NTA solution (Figures 4 and 5); somewhat larger overvoltages are observed for Quadrol and tartrate complexes (Table 1, Figures 4, 6–8)

The comparison of the Cu^{II} reduction rate in the corresponding formaldehyde-free and electroless plating solutions (Figure 2) shows that the most significant acceleration of the Cu^{II} reduction process occurs in the presence of formaldehyde in the potential region -0.5 to -0.8 V in the cases of NTA and Quadrol. The Cu^{II} reduction partial current of -0.4 mA is achieved in these electroless plating solutions in the potential region -0.4 to -0.6 V in the negative-going potential scan (Figures 5 and 6). The rate of cathodic copper deposition becomes similar at the negative potential limit of -0.9 V in both formaldehyde-free and electroless plating solutions (Figure 4). The increase in the rate of Cu^{II} reduction occurs again in the positive-going scan, together with the onset of formaldehyde oxidation (Figures 5 and 6).

The acceleration of the cathodic partial reaction of Cu^{II} reduction in the presence of formaldehyde has been observed in several investigations [7, 16–19] and is

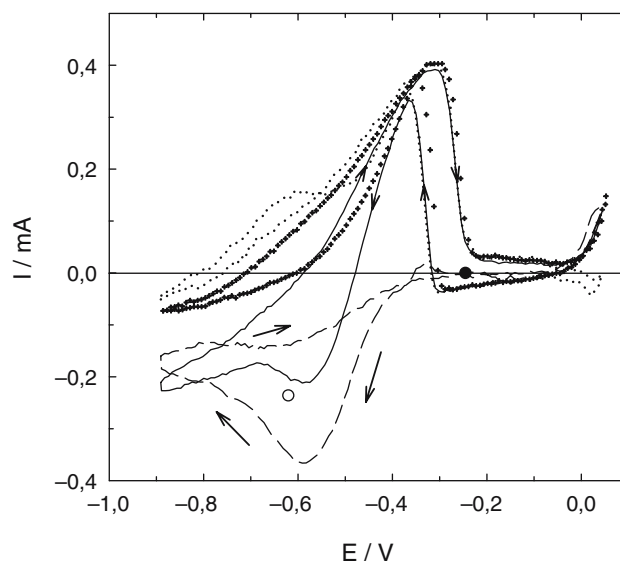


Fig. 6. Dependence of faradaic current [measured directly (—), calculated from EQCM data (- - -), and found from their difference (...)] on copper electrode potential. Solution contained (mol l^{-1}): $\text{CuSO}_4 - 0.008$; $\text{Quadrol} - 0.02$; $\text{CH}_2\text{O} - 0.02$; $\text{pH } 13$; $t^\circ = 20 \pm 1^\circ\text{C}$. (o) – fradaic current measured directly in Cu^{II} -free 0.02 mol l^{-1} formaldehyde solution containing 0.012 mol l^{-1} of Quadrol; (O) – instantaneous copper deposition rate measured by EQCM under open-circuit conditions.

apparently caused by products of formaldehyde oxidation rather than formaldehyde (methyleneglycol or its anion) itself [7, 14]. In electroless copper plating solution, hydrogen evolves on copper as a result of formaldehyde oxidation at more positive potentials than those for cathodic hydrogen evolution in the solutions under study (more negative than -0.9 V in the case of EDTA solution according to DEMS studies) [11]. Possibly, the formation of hydrogen on the copper

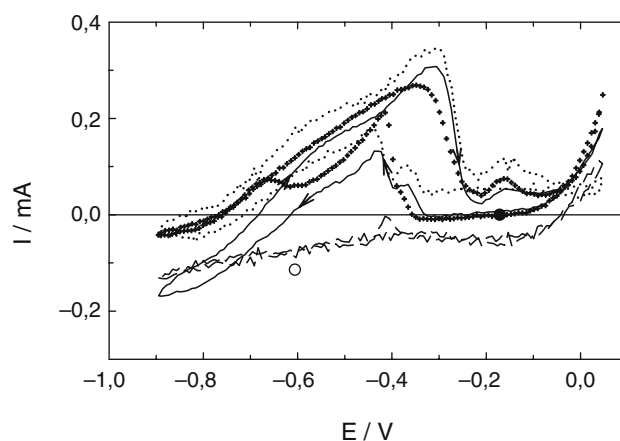


Fig. 7. Dependence of faradaic current [measured directly (—), calculated from EQCM data (- - -), and found from their difference (...)] on copper electrode potential. Solution contained (mol l^{-1}): $\text{CuSO}_4 - 0.008$; $\text{L}(+)\text{-tartrate} - 0.04$; $\text{CH}_2\text{O} - 0.02$; $\text{pH } 13$; $t^\circ = 20 \pm 1^\circ\text{C}$. (o) – fradaic current measured directly in Cu^{II} -free 0.02 mol l^{-1} formaldehyde solution containing 0.032 mol l^{-1} of $\text{L}(+)\text{-tartrate}$; (O) – instantaneous copper deposition rate measured by EQCM under open-circuit conditions.

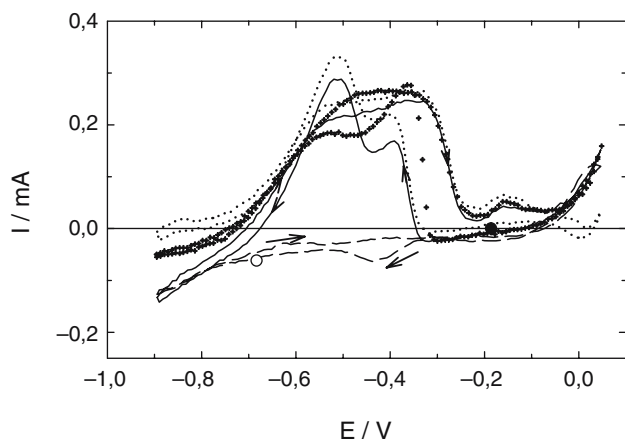


Fig. 8. Dependence of faradaic current [measured directly (—), calculated from EQCM data (- - -), and found from their difference ...] on copper electrode potential. Solution contained (mol l^{-1}): CuSO_4 – 0.008; $\text{DL}(\overline{+})$ -tartrate – 0.04; CH_2O – 0.02; pH 13; $t^\circ = 20 \pm 1$ °C. (o) – faradaic current measured directly in Cu^{II} -free 0.02 mol l^{-1} formaldehyde solution containing 0.032 mol l^{-1} of $\text{DL}(\overline{+})$ -tartrate; (O) – instantaneous copper deposition rate measured by EQCM at open-circuit conditions.

surface at these potentials (–0.4 to –0.8 V) inhibits crystallization of freshly depositing copper atoms, (reaction (3)) and increases the rate of reaction (4). In this case, the overall rate of Cu^{II} reduction (cathodic current) in this particular potential region is determined by the surface concentration of Cu^* .

In $\text{L}(+)$ - and $\text{DL}(\overline{+})$ -tartrate, glycerol and sucrose solutions the presence of formaldehyde has only a small effect on cathodic copper deposition (Figure 4). This difference in copper complex behaviour is probably related to differences in detail of the Cu^{II} reduction mechanism. The tartrate anion interacts with formaldehyde forming cyclic acetal compounds [33, 34] which change the situation at the copper surface and prevents acceleration of copper deposition.

3.3. Formaldehyde oxidation rate in electroless copper plating solutions

The dependence of the formaldehyde oxidation partial current on electrode potential, calculated as the difference between the net current and that found from the EQCM data (Figures 3–6) is similar to that described in

[14]. The occurrence of the anodic current peak in the positive-going scan is determined by Cu_2O formation, leading to decreased catalytic activity of the surface and causing a drop in the partial anodic formaldehyde oxidation current to zero. Anodic current occurring more positively –0.1 V, is due to anodic dissolution of copper, as is evident from the EQCM data. The onset of formaldehyde oxidation during the negative-going potential scan is achieved at ca. –0.3 V, simultaneously with reduction of the inhibiting Cu_2O species. At more negative potentials, the partial current of formaldehyde oxidation diminishes, reaching zero at –0.75 V (Figures 5–8).

Cu^{II} complexing agents affect the CH_2O anodic oxidation rate both in complete plating solution and in Cu^{II} -free formaldehyde solutions. In the second case the CV measurements were carried out after replacing electroless copper plating solutions with alkaline formaldehyde solutions containing the corresponding complexing agent at a concentration equal to that of free (unbound with Co^{II}) complexing agent in the electroless plating solution.

When comparing the voltammograms obtained in Cu^{II} -free solutions in the positive-going scan (the effects of Cu surface oxidation and oxide reduction are involved in the negative-going scans [34, 35]) the onset of CH_2O oxidation for all complexing agents is at ca. –0.75 V, while anodic current depends on the complexing agent: the maximum current at ca. –0.3 V is larger for NTA solutions (ca. 0.6 mA), lower for Quadrol (0.4 mA), and still lower for other 4 complexing agents (ca. 0.3 mA). Though the highest electrocatalytic activity of copper in formaldehyde oxidation is observed for Cu surfaces formed in solutions of Cu^{II} complexes of the lowest stability (NTA), for other ligands the effect of complex stability on Cu electrocatalytic activity is not so clear. A higher electrocatalytic activity of some Cu surfaces could be connected to a higher real surface area and a preferred surface structure formation. A detailed study of these problems is presented in [32].

It is interesting to note that the shape of the CV of anodic formaldehyde oxidation in the case of $\text{L}(+)$ - and $\text{DL}(\overline{+})$ -tartrate solutions is different from other complexing agents both in Cu^{II} -free and complete plating solution (cf. Figures 7, 8 and 5, 6). This may be related

Table 2. Overvoltage (ΔE) of the copper electrode in Cu^{II} complex solutions, determined from EQCM data at a constant copper dissolution or deposition rate of ± 0.5 Hz s^{-1}

Ligand	$\Delta E_a/\text{V}$ Cu–Cu(II) and Cu–Cu(II)– CH_2O systems	$-\Delta E_c/\text{V}$	
		Cu–Cu(II) system	Cu–Cu(II)– CH_2O system
NTA	0.06	0.08	0.03
Sucrose	0.12	0.14*	0.14*
Glycerol	0.13	–	–
$\text{L}(+)$ -tartaric acid	0.12	0.20	0.08
$\text{DL}(\overline{+})$ -tartaric acid	0.10	0.15	0.08
Quadrol	0.15	0.23	0.08

* – ΔE_c determined from EQCM data at copper deposition rate of –1.0 Hz s^{-1} .

to the formation of an acetal-type compound from tartrate and formaldehyde [36, 37].

The rate of formaldehyde oxidation in electroless plating solution is usually similar to that in Cu-free solutions. Some increase in the maximum anodic current in the potential range -0.4 to -0.3 V is observed during the positive-going scan for NTA and L(+)-tartrate solutions (Figures 5 and 7). The behaviour of NTA solutions is different from the others in several aspects: both anodic and cathodic CVs are of more complicated form and in the negative-going scan the maximum anodic current is higher compared to the positive-going scan (Figure 5).

4. Conclusions

The electroless copper deposition rate decreases in the ligand sequence: NTA > Quadrol > glycerol > L(+)-tartrate \sim sucrose > L(+)-tartrate \sim sucrose > DL(±)-tartrate. Both Cu^{II} complex stability and specific ligand effects were found to influence the Cu deposition process. The specific ligand effects are most obvious in the case of Quadrol (high kinetic activity at a high Cu^{II} complex stability), glycerol and sucrose (additional reactions).

According to the EQCM data for 11 Cu^{II} complexes (including data from [14]) the higher kinetic activity is demonstrated by complexes with ligands containing amino groups; the ligand nature is more important for Cu deposition rate than copper complex stability.

The large acceleration of the partial Cu^{II} reduction reaction in complete electroless Cu plating solution was observed for Cu^{II} complexes with NTA and Quadrol, while the CH₂O₂ oxidation rate changed little compared with Cu^{II}-free solutions.

The kinetics of partial reactions and overall electroless Cu deposition can be explained by hypothetical mechanism including intermediate copper oxy-species and active Cu* formation, as well as by the development of the preferred Cu surface structure

References

- G.O. Mallory and J.B. Hajdu (eds.), *Electroless Plating: Fundamentals and Applications* (American Electroplaters and Surface Finishers Society Inc., Orlando, 1990), pp. 539.
- M. Šalkauskas and A. Vaškelis, 'Chemical Metallizing of Plastics' (in Russian) (Khimiya, Leningrad, 1985) 144 pp.
- Vaškelis A. in D. Satas and A.A. Tracton (Eds), 'Coatings Technology Handbook', (Marcel Dekker, New York, 2001), pp. 213–225.
- M. Saito, *J. Metal. Fin. Soc. Jpn.* **16** (1965) 300.
- A. Vaškelis and M. Šalkauskas, *Lietuvos MA Darbai (Proc. Lit. Acad. Sci.)* **B4**(51) (1967) 3(in Russian).
- M. Paunovic, *Plating* **55** (1968) 1161.
- A. Vaškelis and J. Jaciauskiene, *Elektrokhimiya* **17** (1981) 1816(in Russian).
- J.E.A.M. van den Meerakker, *J. Appl. Electrochem.* **11** (1981) 387.
- O. Wolter and J. Heitbaum, *Ber. Bunsen-Ges. Phys. Chem.* **88** (1984) 2.
- Z. Jusys and A. Vaškelis, *Langmuir* **8** (1992) 1230.
- Z. Jusys and A. Vaškelis, *Electrochim. Acta.* **42** (1997) 449.
- A. Vaškelis and Z. Jusys, *Anal. Chim. Acta* **305** (1995) 227.
- Z. Jusys, G. Stalnionis, E. Juzeliunas and A. Vaškelis, *Electrochim. Acta* **43** (1998) 301.
- Z. Jusys, R. Pauliukaitė and A. Vaškelis, *Phys. Chem. Chem. Phys.* **1** (1999) 313.
- R. Schumacher, J.J. Pesek and O.R. Melroy, *J. Phys. Chem.* **8** (1985) 4338.
- H. Wiese and K.G. Weil, *Ber. Bunsen-Ges. Phys. Chem.* **91** (1987) 619.
- B.J. Feldman and O.R. Melroy, *J. Electrochem. Soc.* **136** (1989) 640.
- M. Matsuoka, J. Murai and C. Iwakura, *J. Electrochem. Soc.* **139** (1992) 446.
- A. Bittner, M. Wanner and K.G. Weil, *Ber. Bunsen-Ges. Phys. Chem.* **96** (1992) 647.
- Z. Jusys, H. Massong and H. Baltruschat, *J. Electrochem. Soc.* **146** (1999) 1093.
- G. Rozovskis and A. Vaškelis, *Electroless Copper Plating (in Russian)* (RMTIPI, Vilnius, 1966).
- A. Vaškelis, G. Rozovskis and J. Kulšytė, *Metal Protection* **7** (1971) 558.
- H. Koyano, M. Kato and H. Takenouchi, *J. Electrochem. Soc.* **139** (1992) 3112.
- E. Norkus and A. Vaškelis, *Polyhedron* **13** (1994) 3041.
- E. Norkus, A. Vaškelis, R. Vaitkus and J. Reklaitis, *J. Inorg. Biochem.* **60** (1995) 299.
- E. Norkus, A. Vaškelis, I. Žakaite and J. Reklaitis (1997) *Chemija (Lithuania)* No. 2:16.
- E. Norkus, A. Vaškelis, I. Žakaite and J. Reklaitis, *Talanta* **42** (1995) 1701.
- E. Norkus, A. Vaškelis and I. Žakaite (1996) *Chemija (Lithuania)* No. 3:8.
- A. Vaškelis, G. Stalnionis and Z. Jusys, *J. Electroanal. Chem.* **465** (1999) 142.
- Z. Jusys and G. Stalnionis, *J. Electroanal. Chem.* **431** (1997) 141.
- E. Norkus, A. Vaškelis and I. Stalnioniene, *J. Solid State Electrochem.* **4** (2000) 337.
- A. Vaškelis, E. Norkus, I. Stalnionienė and G. Stalnionis, *Electrochim. Acta* **49** (2004) 1613.
- S. Leopold, J.C. Arrayet, J.L. Bruneel, M. Herranen, J.-O. Carlsson, F. Argoul and L. Servant, *J. Electrochem. Soc.* **150** (2003) C427.
- A. Vaškelis, *Lietuvos MA Darbai (Proc. Lit. Acad. Sci.)* **B4** (1966) 3(in Russian).
- A. Vaškelis, M. Šalkauskas and A. Prokopchik, *Kinetics of Physicochemical Oscillations, Aachen* **3** (1983) 714.
- E. Norkus, A. Vaškelis, E. Butkus and R. Pauliukaitė, *J. Chem. Res. (S)* **N 4** (1997) 126.
- E. Norkus, R. Pauliukaitė and A. Vaškelis, *Pol. J. Chem.* **73** (1999) 1837.